Physics Letters A ••• (••••) •••–•••

Contents lists available at ScienceDirect

Physics Letters A

www.elsevier.com/locate/pla

Electro-optic tunable band-stop filters using piezoelectric superlattices

Zheng-Hua Tang [a], Zheng-Sheng Jiang [b], Tao Chen [c], Da-Jun Lei [a], Jian-Quan Huang [a], Feng Qiu [a], Chun-Zhi Jiang [a], Min Yao [a,*], Xiao-Yi Huang [a]

[a] Xiangnan University-Gospell Joint Laboratory of Microwave Communication Technology, Xiangnan University, Chenzhou 423000, China
[b] National Laboratory of Solid State Microstructures and Department of Physics, Nanjing University, Nanjing 210093, China
[c] School of Physical, Environmental and Mathematical Sciences, University of New South Wales at ADFA, Canberra, ACT 2600, Australia

ARTICLE INFO

Article history:
Received 26 March 2018
Received in revised form 12 July 2018
Accepted 24 July 2018
Available online xxxx
Communicated by R. Wu

Keywords:
The band stop filter
Electro-optic effect
Band structures

ABSTRACT

A novel band-stop filter, which uses the piezoelectric superlattices with the external direct-current (DC) electric fields, is presented. The forbidden band of the band-stop filter can be generated by the coupling between lattice vibration and electromagnetic waves and can be tuned continuously and reversibly by the DC electric field via the electro-optic effect. The band structures and transmission spectra of the band-stop filter show that the relative bandwidth of forbidden bands will be increased from 0.43% to 26.2% and their sizes can be broadened from 0.043 GHz to 2.98 GHz when the DC electric field is increased from 0 to 1.343×10^6 V/m. The bandwidth tunability by the electro-optic effect provides a good guidance for the filter design that works in broadband frequencies.

1. Introduction

The band-stop filter (BSF) possessing the characteristic that electromagnetic waves at specific frequencies are attenuated to a very low level. They have attracted great attention in recent years because of potential applications in the communication field. Currently, a variety of BSFs have been investigated which involve a conductive rubber split-ring resonator [1], a barium hexagonal ferrite film strip [2], graphene structures [3,4], a coupled cut-wire pair nanostructure [5], a THz metamaterials structure [6], compact microstrip structures [7–9], metal-insulator-metal structures [10–14], 3-dimensional frequency selective surfaces [15] and a self-complementary metasurface [16]. The general construction for the BSFs is to control and manipulate the surface plasmons [17] which originate from the resonant interaction between the charge oscillation of metal surface and the electromagnetic field of electromagnetic waves propagating along the interface of metal and dielectric materials. The surface plasmon standing waves can be formed and the surface plasmon-stop band is opened because the surface plasmon modes can be scattered by constructing appropriate nanostructures. The resonant nature of these structures to electromagnetic waves lead to narrow bandwidth of the BSFs, which greatly reduces the scope of applications of wider stop-bands. The bandwidth tunability of the BSFs is also mainly based on their structural reconfiguration. This also means that the bandwidth adjustment is not continuous and reversible.

To overcome the narrow bandwidth and irreversibility of bandwidth adjustment of current BSFs, an alternative approach to constructing the BSF is to explore the piezoelectric superlattices, which can generate the forbidden band because of the intersection and hybridization of the folded phonon branches and the photon branch in piezoelectric superlattices [18–20] due to periodic modulation of piezoelectric coefficient in these structures themselves. Although many investigations with respect to the BSFs have been carried out so far, the research on the BSF with piezoelectric superlattices, especially using the electro-optic effect as a way to modulate its bandwidth, is still rare to the best of my knowledge. The BSF is constructed by piezoelectric superlattices with ferroelectric domains with electric polarization along $\pm z$-axis and an applied DC electric field along the same axis as the polarization and is shown in Fig. 1. There are three key points with respect to the BSF that need to be emphasized, as follows. (1) The BSF using piezoelectric superlattice has a small footprint and its size is about 1 cm in our design, which lead it to be easily integrated into microwave devices or systems. (2) The relative bandwidth of the forbidden band of the BSF is widened from 0.43% to 25.2% with the DC electric field increased from 0 to 1.342×10^6 V/m and the corresponding maximum absolute bandwidth is about 2.88 GHz for the structure with $L_{P+} = L_{P-} = 1.38$ μm. (3) The bandwidth tunability of the BSF by an external DC electric field via the electro-optic effect is continuous and reversible.

* Corresponding author.
E-mail address: 369084915@qq.com (M. Yao).

https://doi.org/10.1016/j.physleta.2018.07.040
0375-9601/

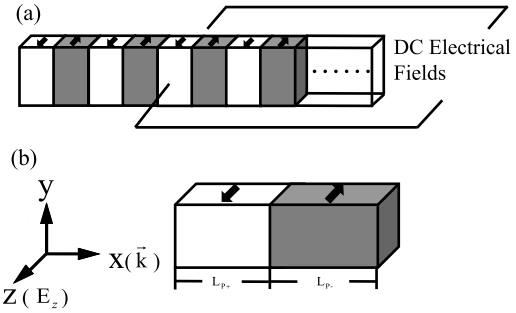

Fig. 1. A schematic diagram of the band-stop filter using piezoelectric superlattices with an external DC electric field along the z-axis (a) and a minimum period of the BSF (b). The piezoelectric domains with polarization along the $\pm z$-axis are represented by the white and gray blocks, respectively. The wavevector k is along the x-axis. The thicknesses of domains are set as $L_{P+} = L_{P-} = 1.38$ μm.

The rest of this paper is organized as follows: In Section 2, the brief descriptions of the BSF are presented, and the experimental setting for them is sketched. In addition, the corresponding fundamental dynamic equations for the piezoelectric domains with the electro-optic effect are derived. In Section 3, the band structure and transmission spectra for the BSF under external electric fields are numerically computed by the transfer matrix method and the corresponding results are analyzed. In particular, the relative bandwidth of the forbidden bands is discussed in detail. Our conclusion is presented in Section 4.

2. The experimental configuration and dynamical equations

In this paper, we consider the band-stop filter using piezoelectric superlattices as shown in Fig. 1. The BSF is constructed by a two-step process: (1) two piezoelectric domains ($L_{p+} = L_{p-} =$ 1.38 μm) with opposite polarizations form a basic structural unit and the unit is repeatedly arranged in the x-axis direction. (2) an external dc electric field along the z-axis is applied to this structure. Owing to the transverse dimension of the BSF is smaller than its longitudinal size, the BSF can be treated as a one-dimensional structure. A ferroelectric PZT compound selected as the piezoelectric domains is manly based on complete material parameters [21] available, the large electro-optic effect [22] and the high coercive field [23]. As in the situation in Fig. 1, the polarization of piezoelectric domains of the BSF is along ±z-axis and the external DC electric field along z-axis is also applied to the BSF. The lattice period is $L = L_{P+} + L_{P-}$, with L_{P+} and L_{P-} denoting the layer thicknesses of piezoelectric domains along $\pm z$-axis polarization, respectively. The reason for such a choice is that this structure can ensure electromagnetic waves propagating along the BSF modulated by piezoelectric effect and freely tunable bandwidth of stop band of BSF by an external DC field occurring. Consider an electromagnetic wave impinging on the BSF, the longitudinal acoustic wave coupling to the electromagnetic wave can occur.

The experimental setting we consider determines that the components of transverse magnetic field $H_y(x,t)$, transverse electric field $E_y(x,t)$ and longitudinal lattice displacement $u_x(x,t)$ are nonzero. The dynamic properties of this structure can be described by the coupled Maxwell equations and the lattice vibration equation which are given by

$$\frac{\partial}{\partial z}E_z(x,t) = \frac{\partial}{\partial t}B_y(x,t), \tag{1}$$

$$\frac{\partial}{\partial z}H_y(x,t) = \frac{\partial}{\partial t}D_z(x,t), \tag{2}$$

$$\rho\frac{\partial^2}{\partial t^2}u_x(x,t) = \frac{\partial}{\partial z}Z_1(x,t), \tag{3}$$

with $B_y(x,t)$ representing the magnetic induction along the y-axis, $D_z(x,t)$ denoting the electric displacement along the z-axis and $Z_1(x,t)$ denoting the stress component along the x-axis. ρ denotes the mass density. Combining the specific forms of dielectric, piezoelectric and electro-optic tensors [24–26] of PZT domains with polarization along the z-axis, we can easily write the equations describing the electric displacement $D_z(x,t)$, the magnetic induction $B_y(x,t)$, and strain components e_1, e_2 and e_3, as follows.

$$\begin{aligned} D_z(x,t) &= d_{31}(x)Z_1(x,t) + d_{32}(x)Z_2(x,t) + d_{33}(x)Z_3(x,t) \\ &\quad + \epsilon_0\epsilon_{33}E_z(x,t) - \epsilon_0\gamma_{33}\epsilon_{33}^2E_z^0E_z(x,t), \end{aligned} \tag{4}$$

$$\begin{aligned} e_1(x,t) &= s_{11}Z_1(x,t) + s_{12}Z_2(x,t) + s_{13}Z_3(x,t) \\ &\quad + d_{31}(x)E_z(x,t), \end{aligned} \tag{5}$$

$$\begin{aligned} e_2(x,t) &= s_{21}Z_1(x,t) + s_{22}Z_2(x,t) + s_{23}Z_3(x,t) \\ &\quad + d_{32}(x)E_z(x,t), \end{aligned} \tag{6}$$

$$\begin{aligned} e_3(x,t) &= s_{31}Z_1(x,t) + s_{32}Z_2(x,t) + s_{33}Z_3(x,t) \\ &\quad + d_{33}(x)E_z(x,t). \end{aligned} \tag{7}$$

Here, $d_{3j}(x)(j = 1,2,3)$ represent the piezoelectric coefficient components. To emphasize the reversal of domains periodic polarization, they are written as the function of space. ϵ_0 denotes the dielectric constant in vacuum and ϵ_{33} denotes the relative dielectric constant. γ_{33} denotes the electro-optic coefficient and E_z^0 represents the DC electric field along the z-axis. The components of elastic compliance tensor are represented by s_{ij} $(i,j = 1,2,3)$. The experimental configuration shown in Fig. 1 determines the strain component $e_1 = \partial u_x(x,t)/\partial x$ and components $e_2 = e_3 \equiv 0$. $u_x(x,t)$ denotes the x-component of lattice displacement. K denotes the symmetrical bulk modulus tensor and is defined as the inverse matrix of elastic compliance tensor. Substituting the components K, e_1, e_2 and e_3 into Eqs. (4)–(7), one arrives at

$$\begin{aligned} D_z(x,t) &= [d(x)K]_{31}\partial u_x(x,t)/\partial x + \epsilon_0(\epsilon_{33} - \Delta\epsilon_{33} \\ &\quad - \gamma_{33}\epsilon_{33}^2E_z^0)E_z(x,t), \end{aligned} \tag{8}$$

$$B_z(x,t) = \mu_0\mu_{33}H_z(x,t), \tag{9}$$

$$Z_1(x,t) = K_{11}\partial u_x(x,t)/\partial x - [d(x)K]_{31}E_y(x,t). \tag{10}$$

μ_0 is the permeability in vacuum and μ_{33} is the relative permeability. The matrix representations $[d(x)K]_{ij} = \sum_{k=1}^{3} d_{ik}(x)K_{kj}$ and $\Delta\epsilon_{33} = (dKd^T)_{33}/\epsilon_0$ are introduced to have compact notations and the latter is one of the corrections to the relative dielectric constant of the compound PZT. The dynamical equations describing the property of the piezoeletric domains are given by

$$\begin{aligned} \left(\frac{\omega L}{2\pi c_s}\right)\bar{E}_z(\bar{x},\omega) &= i\alpha_1\frac{\partial}{\partial\bar{x}}\bar{H}_y(\bar{x},\omega) \\ &\quad + \beta_1\left(\frac{\omega L}{2\pi c_s}\right)\theta(\bar{x})\frac{\partial}{\partial\bar{x}}\bar{u}_x(\bar{x},\omega), \end{aligned} \tag{11}$$

$$\left(\frac{\omega L}{2\pi c_s}\right)\bar{H}_y(\bar{x},\omega) = i\alpha_2\frac{\partial}{\partial\bar{x}}\bar{E}_z(\bar{x},\omega), \tag{12}$$

$$\begin{aligned} \left(\frac{\omega L}{2\pi c_s}\right)^2\bar{u}_x(\bar{x},\omega) &= -\frac{\partial^2}{\partial\bar{x}^2}\bar{u}_x(\bar{x},\omega) \\ &\quad + \frac{\partial}{\partial\bar{x}}[\theta(\bar{x})\bar{E}_z(\bar{x},\omega)]. \end{aligned} \tag{13}$$

A set of dimensionless functions $x = \bar{x}L/2\pi$, $\bar{H}_y(x,t) = \sqrt{\mu_0/\bar{K}_{11}}H_y(x,t)$, $u_x(x,t) = \bar{u}_x(x,t)L/2\pi$, $\bar{E}_z(x,t) = \bar{d}_{31}(\bar{x})E_z(x,t)$ are introduced to give the dimensionless form of Eqs. (11)–(13) in order to facilitate the calculation. $\bar{d}_{31}(\bar{x}) = \bar{d}_{31}\theta(\bar{x})$ is explored

Please cite this article in press as: Z.-H. Tang et al., Electro-optic tunable band-stop filters using piezoelectric superlattices, Phys. Lett. A (2018), https://doi.org/10.1016/j.physleta.2018.07.040